

## Symplectic *ab initio* no-core shell model

J.P. Draayer, T. Dytrych, K.D. Sviratcheva, and C. Bahri

*Department of Physics and Astronomy,  
Louisiana State University, Baton Rouge,  
LA 70803, USA.*

J.P. Vary

*Department of Physics and Astronomy,  
Iowa State University, Ames,  
IA 50011, USA.*

Recibido el 28 de febrero de 2008; aceptado el 7 de mayo de 2008

The present study confirms the significance of the symplectic  $Sp(3, \mathbb{R})$  symmetry in nuclear dynamics as unveiled, for the first time, by examinations of realistic nucleon-nucleon ( $NN$ ) interactions as well as of eigenstates calculated in the framework of the *ab initio* No-Core Shell Model (NCSM). The results reveal that the NCSM wave functions for light nuclei highly overlap (at the  $\sim 90\%$  level) with only a few of the most deformed  $Sp(3, \mathbb{R})$ -symmetric basis states. This points to the possibility of achieving convergence of higher-lying collective modes and reaching heavier nuclei by expanding the NCSM basis space beyond its current limits through  $Sp(3, \mathbb{R})$  basis states. Furthermore, the symplectic symmetry is found to be favored by the JISP16 and CD-Bonn realistic nucleon-nucleon interactions, which points to a more fundamental origin of the symplectic symmetry.

*Keywords:* Shell model; nucleon-nucleon interactions; models based on group theory.

En el presente trabajo se confirma la importancia de la simetría simpléctica  $Sp(3, \mathbb{R})$  en la dinámica nuclear a través de estudios de interacciones nucleón-nucleón realistas así como de eigenestados calculados en el marco del modelo de capas sin carozo (NCSM, por sus siglas en inglés). Los resultados demuestran para núcleos ligeros un gran traslapeo entre las funciones de onda NCSM usando nada más los estados base con simetría  $Sp(3, \mathbb{R})$  con mayor deformación, lo cual abre la posibilidad para obtener convergencia de modos colectivos con energías altas y poder describir núcleos más pesados con una extensión del espacio de los estados base NCSM usando estados con simetría  $Sp(3, \mathbb{R})$ . Además, las interacciones nucleón-nucleón realistas JISP16 y CD-Bonn favorecen la simetría simpléctica lo cual apunta a una explicación a nivel más fundamental de la simetría simpléctica.

*Descriptor:* Modelo de capas; interacciones nucleón-nucleón; modelos con base en teoría de grupos.

PACS: 21.60.Cs; 13.75.Cs; 21.60.Fw

### 1. Introduction

Group-theoretical approaches, which exploit the underlying symmetries of nuclear dynamics, have been proved successful in reproducing striking spectral features of atomic nuclei, such as pairing gaps in nuclear energy spectra or enhanced electric quadrupole transitions in collective rotational bands. For example, the rotational nature of the ground-state band in  $^{12}\text{C}$  nucleus has long been recognized, and early-on group-theoretical methods with  $SU(3)$  serving as the underpinning (sub-) symmetry were used in its description. Symplectic algebraic approaches ( $Sp(3, \mathbb{R}) \supset SU(3) \supset SO(3)$ ) have achieved a very good reproduction of low-lying energies and  $B(E2)$  values in light nuclei [1-3] and specifically in  $^{12}\text{C}$  using phenomenological interactions [4] or truncated symplectic basis with simplistic (semi-) microscopic interactions [5,6]. Recently, mean-field calculations confirm the significant role of the  $Sp(3, \mathbb{R})$  symmetry for a description of the second and third  $0^+$  highly-deformed states in  $^{16}\text{O}$  and their rotational bands [7]. Now, for the first time, we establish the dominance of the symplectic  $Sp(3, \mathbb{R})$  symmetry in light nuclei as unveiled through *ab initio* No-Core Shell Model (NCSM) calculations starting with realistic nucleon-nucleon

( $NN$ ) interactions tied to quantum chromodynamics (QCD). Such a comparison with results from the *ab initio* NCSM approach, which builds upon a ‘first principles’ foundation, points to the possibility of employing the  $Sp(3, \mathbb{R})$  shell model for a fully microscopic description emerging from a fundamental interaction linked to the well-known properties of the two and three-nucleon systems.

Particularly, our ‘proof-of-principle’ study [8] reveals a significant large overlap ( $\sim 85 - 90\%$ ) of only a few  $Sp(3, \mathbb{R})$  irreps with the NCSM wave functions for low-lying states in  $^{12}\text{C}$  and  $^{16}\text{O}$  together with the close reproduction of the  $B(E2 : 2_1^+ \rightarrow 0_{gs}^+)$  NCSM estimates. In addition, we find that realistic nucleon-nucleon interactions that reproduce  $NN$  phase shifts, such as the JISP16 (used to calculate the NCSM eigenstates) and the CD-Bonn (one-boson-exchange potential), respect the symplectic  $Sp(3, \mathbb{R})$  symmetry and the complementary (spin-isospin) supermultiplet symmetry to a considerably large degree. This manifestation of the symplectic symmetry at the nucleon-nucleon level and in the many-body dynamics of light nuclei points to the propensity of nucleon-nucleon interactions toward preserving the  $Sp(3, \mathbb{R})$  symmetry and suggests that, in turn, the nuclear many-body system acts as a filter that allows the symplectic

symmetry to propagate in a coherent way into the many-body dynamics while reducing the effects of any symplectic symmetry breaking terms.

The *ab initio* symplectic no-core shell model (Sp-NCSM) holds promise to reach new domains of nuclear structure by expanding the conventional harmonic oscillator basis in terms of the symmetry-adapted and physically relevant symplectic basis. The Sp-NCSM approach augments the NCSM concept by recognizing that the choice of coordinates, especially when deformed nuclear shapes dominate, is crucial and presents a solution in terms of coordinates that reflect symmetries inherent to nuclear systems. Hence, major reductions (many orders of magnitude) in model space requirements can be achieved. In addition, the  $\text{Sp}(3, \mathbb{R})$  symmetry properties of the nucleon-nucleon interaction make possible the use of algebraic methods and even analytic solutions when the  $\text{Sp}(3, \mathbb{R})$  symmetry-adapted basis is utilized. In particular, the symplectic extension of the NCSM will allow one to account for even higher  $\hbar\Omega$  configuration required to realize experimentally measured B(E2) values without an effective charge, and to accommodate highly deformed spatial configurations including  $\alpha$ -cluster structures [9], which are beyond the reach of traditional NCSM calculations but are essential for modeling, *e.g.*, the second  $0^+$  state in  $^{12}\text{C}$  (the ‘Hoyle’ state of astrophysical interest) as well as in  $^{16}\text{O}$ .

## 2. Symplectic symmetry in many-body nuclear dynamics

The significance of the symplectic symmetry [10] emerges from the physical relevance of its 21 generators, which are directly related to the particle momentum ( $p_{s\alpha}$ ) and coordinate ( $q_{s\beta}$ ) operators and constructed as

$$\sum_s p_{s\alpha} p_{s\beta}, \quad \sum_s (q_{s\alpha} p_{s\beta} \pm q_{s\beta} p_{s\alpha}), \quad \sum_s q_{s\alpha} q_{s\beta}$$

with  $\alpha, \beta = x, y,$  and  $z$  for the 3 spatial directions and  $s$  labeling an individual nucleon. These generators realize important observables, such as the many-particle kinetic energy  $\sum_{s,\alpha} p_{s\alpha}^2/2m$ , the mass quadrupole moment and angular momentum operators, together with multi-shell collective vibrations and vorticity degrees of freedom for a description of rotational dynamics in a continuous range from irrotational to rigid rotor flow.

Alternatively, the elements of the  $\mathfrak{sp}(3, \mathbb{R})$  algebra can be represented as bilinear products in harmonic oscillator (HO) raising

$$b_\alpha^\dagger = \sqrt{\frac{m\Omega}{2\hbar}} x_\alpha - i \sqrt{\frac{1}{2m\hbar\Omega}} p_\alpha$$

and lowering ( $b_\alpha$ ) operators. In this realization, the natural set of the translationally invariant symplectic generators includes the HO Hamiltonian

$$H_0^{(00)} = \sqrt{3} \sum_{s=1}^A [b_s^\dagger \times b_s]^{(00)} - \frac{\sqrt{3}}{A} \sum_{s,t=1}^A [b_s^\dagger \times b_t]^{(00)} + \frac{3}{2}(A-1),$$

which counts the total number of oscillator bosons, together with,

$$\begin{aligned} A_{LM}^{(20)} &= \frac{1}{\sqrt{2}} \sum_s [b_s^\dagger \times b_s^\dagger]_{LM}^{(20)} - \frac{1}{\sqrt{2A}} \sum_{s,t} [b_s^\dagger \times b_t^\dagger]_{LM}^{(20)} \\ B_{LM}^{(02)} &= \frac{1}{\sqrt{2}} \sum_s [b_s \times b_s]_{LM}^{(02)} - \frac{1}{\sqrt{2A}} \sum_{s,t} [b_s \times b_t]_{LM}^{(02)} \\ C_{LM}^{(11)} &= \sqrt{2} \sum_s [b_s^\dagger \times b_s]_{LM}^{(11)} - \frac{\sqrt{2}}{A} \sum_{s,t} [b_s^\dagger \times b_t]_{LM}^{(11)}, \end{aligned} \quad (1)$$

where  $A_{LM}^{(20)}$  are six symplectic raising operators that induce a 2-shell ( $2\hbar\Omega$ ) 1p-1h monopole ( $L=0$ ) or quadrupole ( $L=2$ ) excitation (*i.e.* one particle raised by two harmonic oscillator shells) together with a smaller  $2\hbar\Omega$  2p-2h (two particles raised by one shell each) correction for eliminating the spurious center-of-mass motion,  $B_{LM}^{(02)}$  are symplectic lowering operators ( $= (A_{LM}^{(20)})^\dagger$ ), and  $C_{LM}^{(11)}$  are eight traceless single-shell  $\text{SU}(3)$  generators.

The  $\text{Sp}(3, \mathbb{R})$ -symmetric structure divides the full space into multi-shell (vertical) slices, called symplectic  $\text{Sp}(3, \mathbb{R})$  irreducible representations (irreps), each of which is built over a symplectic bandhead and can extend to very high  $\hbar\Omega$  spaces. For a  $\sigma \equiv N_\sigma (\lambda_\sigma \mu_\sigma) \text{Sp}(3, \mathbb{R})$  irrep and

$$n(\omega) \equiv N_{n(\omega)} (\lambda_{n(\omega)} \mu_{n(\omega)}),$$

the  $\text{Sp}(3, \mathbb{R})$ -symmetric basis states,

$$|\sigma n \rho \omega \kappa (LS) J M_J\rangle = \left[ \mathcal{P}^n (A^{(20)}) \times |\sigma\rangle \right]_{\kappa (LS) J M_J}^{\rho \omega}, \quad (2)$$

are constructed by acting with multiples of the symplectic raising operator,  $A^{(20)}$ , on a set of basis states of the symplectic bandhead (define by  $B^{(02)}|\sigma\rangle = 0$ ). Note that, *e.g.*, a 0p-0h  $\text{Sp}(3, \mathbb{R})$  irrep includes 0p-0h nuclear configuration of the  $|\sigma\rangle$  bandhead together with single- and multi-particle excitations built upon these configurations.<sup>i</sup> The quantum number  $N_\omega = N_\sigma + N_n$  is the total number of oscillator quanta related to the eigenvalue,  $N_\omega \hbar\Omega$ , of a HO Hamiltonian that is free of spurious modes. The  $(\lambda_n \mu_n)$  set gives the overall  $\text{SU}(3)$  symmetry of  $N_n/2$  coupled raising operators in the  $\mathcal{P}$  polynomial and  $(\lambda_\omega \mu_\omega)$  specifies the  $\text{SU}(3)$  symmetry of the symplectic state. In accordance with the mapping [11] between the shell-model  $(\lambda \mu) \text{SU}(3)$  labels

TABLE I. Overlaps of NCSM eigenstates ( $\hbar\Omega = 15$  MeV,  $6\hbar\Omega$  model space) for the  $0_{gs}^+, 2_1^+$ , and  $4_1^+$  states in  $^{12}\text{C}$  and the  $0_{gs}^+$  in  $^{16}\text{O}$  with the few dominant  $\text{Sp}(3, \mathbb{R})$  irreps built over  $0\hbar\Omega$  0p-0h (and  $2\hbar\Omega$  2p-2h) bandheads.

Type of $\text{Sp}(3, \mathbb{R})$ bandheads	$^{12}\text{C}$			$^{16}\text{O}$
	$0_{gs}^+$	$2_1^+$	$4_1^+$	$0_{gs}^+$
$0\hbar\Omega$ 0p-0h	82.28%	81.42%	79.21%	75.91%
$0\hbar\Omega$ 0p-0h+ $2\hbar\Omega$ 2p-2h	87.19%	86.16%	84.08%	85.85%

and the shape variables of the Bohr-Mottelson collective model [12], namely, the prolate elongation  $\beta > 0$  and the  $0 \leq \gamma \leq \pi/2$  asymmetry parameter, the symplectic basis states bring forward important information about the nuclear shapes and deformation in terms of their  $(\lambda_\omega \mu_\omega)$   $SU(3)$  symmetry (2). For example,  $(\lambda_\omega 0)$  and  $(0 \mu_\omega)$  describe prolate ( $\gamma \sim 0^\circ$ ) and oblate ( $\gamma \sim 60^\circ$ ) shapes, respectively, with increasing  $\lambda_\omega$  ( $\mu_\omega$ ) toward larger deformations,  $\beta$ .

The  $0_{gs}^+$  ground state and the lowest  $2^+(\equiv 2_1^+)$  and  $4^+(\equiv 4_1^+)$  states of the deformed  $^{12}\text{C}$  nucleus and the lowest-lying  $0^+$  states of the ‘‘closed-shell’’  $^{16}\text{O}$  nucleus were calculated using the NCSM as implemented through the Many Fermion Dynamics (MFD) code [13] with an effective interaction derived from the realistic JISP16  $NN$  potential [14] for different  $\hbar\Omega$  oscillator strengths and with the bare interaction. These states were analyzed for their symplectic symmetry structure by projecting the NCSM wave functions onto the symplectic model subspace. The results show that for these states there are only a few important  $0p-0h$  and  $2\hbar\Omega$   $2p-2h$  symplectic configuration in the  $N_{\max} = 6$  ( $6\hbar\Omega$  model space) [8] that constitute as much as 85-90% of the NCSM eigenstates (Table I). As  $N_{\max}$  is increased the dimension of the  $J = 0, 2$ , and 4 symplectic space built on the  $0p-0h$   $Sp(3, \mathbb{R})$  bandheads grows very slowly compared to the NCSM space dimension (Table II) [15]. The net result is that as  $N_{\max}$  increases the symplectic model subspace is an ever smaller fraction of the NCSM basis space, even when the most dominant  $2\hbar\Omega$   $2p-2h$   $Sp(3, \mathbb{R})$  irreps are included [8]. The reduction is even more dramatic in the case of  $^{16}\text{O}$ , where only the  $J = 0$  symplectic space can be taken into account for the  $0^+$  states under consideration (Table II). This means that the space spanned by the set of relevant symplectic basis states is computationally manageable even when high- $\hbar\Omega$  configuration are included. Of course, if one were to include all possible  $N\hbar\Omega$   $kp-kh$  starting state configuration in the ( $N \leq N_{\max}$ ) space, and allowed multiples thereof, one would span the full NCSM model space.

In the case of  $^{12}\text{C}$ , approximately 84-87% of the NCSM eigenstates fall within a subspace spanned by the most significant three  $0p-0h$  and twenty  $2\hbar\Omega$   $2p-2h$   $Sp(3, \mathbb{R})$  irreps (Table I). (Note that for these states  $4\hbar\Omega$   $4p-4h$  symplectic irreps are found to be negligible.) As one varies the  $\hbar\Omega$  oscillator strength, the projection changes slightly reaching close to 90% for  $\hbar\Omega = 11$  MeV [8].

TABLE II. Model-space dimensions for different  $N_{\max}$  cutoff values for the NCSM and the 3 most significant  $0p-0h$   $Sp(3, \mathbb{R})$  irreps limited to  $J = 0, 2$ , and 4 states in  $^{12}\text{C}$  as well as the one and only  $0p-0h$   $Sp(3, \mathbb{R})$  irrep with  $J = 0$  in  $^{16}\text{O}$ .

		$0\hbar\Omega$	$4\hbar\Omega$	$8\hbar\Omega$	$12\hbar\Omega$
$^{12}\text{C}$	NCSM	51	$1.12 \times 10^6$	$5.94 \times 10^8$	$8.08 \times 10^{10}$
	3 $Sp(3, \mathbb{R})$ irreps	13	216	1030	2979
$^{16}\text{O}$	NCSM	1	$3.44 \times 10^5$	$9.70 \times 10^8$	$3.83 \times 10^{11}$
	1 $Sp(3, \mathbb{R})$ irrep	1	4	11	23

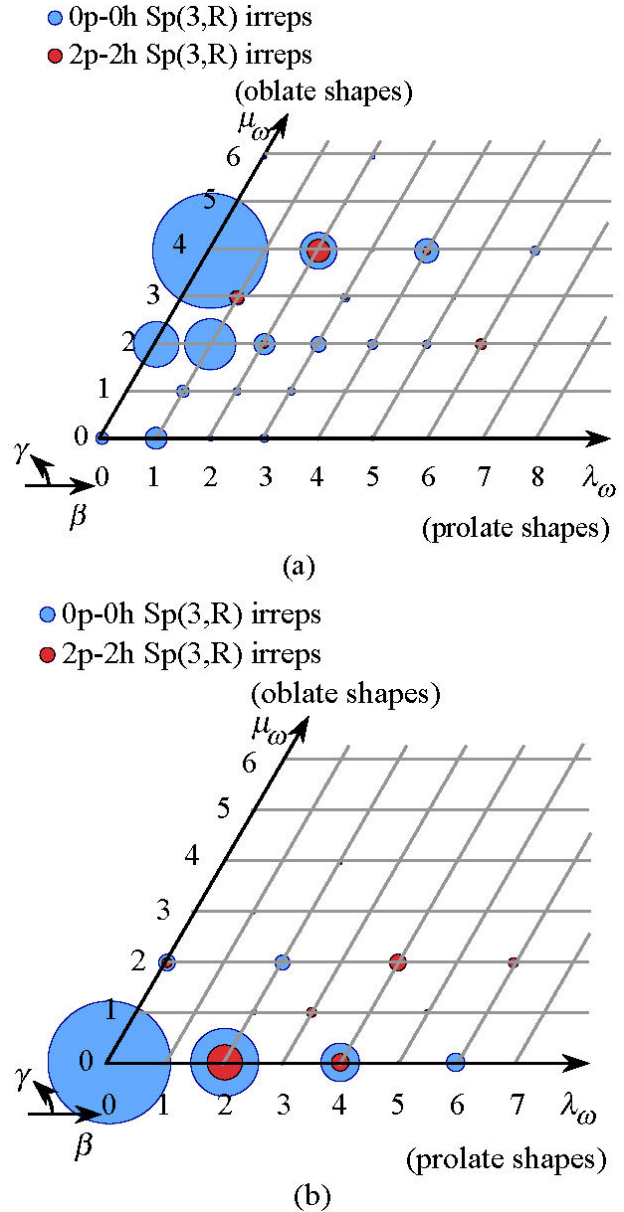


FIGURE 1. Probability (amplitude squared as indicated by the area of the circles) for the symplectic states which make up the most important  $0p-0h$  (blue) and  $2\hbar\Omega$   $2p-2h$  (red) symplectic irreps, within the NCSM ground state in (a)  $^{12}\text{C}$  and (b)  $^{16}\text{O}$ ,  $\hbar\Omega = 15$  MeV. The  $Sp(3, \mathbb{R})$  states are grouped according to their  $(\lambda_\omega \mu_\omega)$   $SU(3)$  symmetry, which is mapped onto the  $(\beta \gamma)$  shape variables of the collective model.

As expected for the  $^{12}\text{C}$  ground state rotational band, oblate shapes dominate, especially among the  $0\hbar\Omega$  components (Fig. 1a). The significance of the most important  $(24)$  and  $(13)$   $2\hbar\Omega$   $2p-2h$  symplectic irreps, in addition to the  $0p-0h$   $Sp(3, \mathbb{R})$  irrep contribution, clearly indicate a propensity of the  $2\hbar\Omega$  components in the NCSM ground state band towards oblate deformed shapes. However, it is interesting to note that the most prolate deformed configuration is also present as indicated by a non-zero projection onto the  $(62)$  symplectic bandhead. The symplectic excitations above the

relevant  $\text{Sp}(3, \mathbb{R})$  bandheads point to the development of a more complex shape structure as seen, for example, in Fig. 1a for the  $^{12}\text{C}$  ground state. Among these, the stretched symplectic states appear to be of a special interest as they usually possess larger overlaps with the realistic states under consideration as compared to the other symplectic excitations. The stretched states are those with  $\mu_\omega = \mu_\sigma$  and maximum value of  $\lambda_\omega$ , namely  $\lambda_\sigma + N_n$  for  $N_n \hbar\Omega$  excitations above the symplectic bandhead. These correspond to horizontal (same  $\mu_\omega$ ) increments of two  $\lambda_\omega$  units in the plane of Fig. 1 starting from the bandhead configuration

For  $^{16}\text{O}$ , the single  $0p\text{-}0h (00)S = 0 \text{Sp}(3, \mathbb{R})$  irrep realizes 75 – 80% of the NCSM realistic wave function. The  $0\hbar\Omega$  projection of the  $0p\text{-}0h$  irrep (around 40 – 55% for values of the oscillator strength  $\hbar\Omega = 12 \text{ MeV}$  to  $16 \text{ MeV}$  [15]) reflect the spherical shape preponderance in the  $^{16}\text{O}$  ground state (Fig. 1b). In addition, a relatively significant mixture of slightly prolate deformed shapes are observed and they are predominantly associated with stretched symplectic excitation states (along the horizontal  $\lambda_\omega$  axis in Fig. 1b). Overall, the ground state in  $^{16}\text{O}$  as calculated by NCSM projects at the 85%-90% level onto the  $J = 0$  symplectic symmetry-adapted basis (Table I) with a total dimensionality of only  $\approx 0.001\%$  of the NCSM space [8].

### 3. Nucleon-nucleon interactions and symplectic symmetry

The large overlap ( $\sim 85 - 90\%$ ) of only a few  $\text{Sp}(3, \mathbb{R})$  irreps with the NCSM wave functions for low-lying states in  $^{12}\text{C}$  and  $^{16}\text{O}$  together with the close reproduction of the  $B(E2 : 2_1^+ \rightarrow 0_{gs}^+)$  NCSM estimates point to the manifestation of the symplectic symmetry in the low-lying structure of these nuclei. Furthermore, as shown in Ref. 8, the  $\text{Sp}(3, \mathbb{R})$  symmetry structure and hence the geometry of the nucleon system being described is nearly independent of the  $\hbar\Omega$  oscillator strength. The symplectic symmetry also dominates the non-zero spin parts of the NCSM wave functions for  $^{12}\text{C}$  as well as  $^{16}\text{O}$  regardless of whether the bare or the effective interactions are used. This points to a more fundamental origin of the symplectic symmetry, one that goes beyond finite space truncation and its compensation by renormalization of the bare interaction.

We searched for selected underlying symmetries in the JISP16 and CD-Bonn realistic interactions using spectral distribution theory [16,17] a theory that has also been used in recent applications in quantum chaos, nuclear reactions and nuclear astrophysics with studies on nuclear level densities, transition strength densities, and parity/time-reversal viola-

tion (for example, see Ref. 18). This is done by evaluating the correlation between the  $NN$  interactions and a  $\text{Sp}(3, \mathbb{R})$  symmetry-respecting microscopic model interaction. As these symmetries are clearly important for certain spectral features, we have a tool for rapidly assessing the likely success of the  $NN$  interactions for reproducing those spectral features. Literally the correlation coefficient is a measure of the extent to which two interactions “look like” (are correlated with) one another.

The significance of the spectral distribution method is related to the fact that low-order energy moments over a certain domain of single-particle states, such as the energy centroid of an interaction (its average expectation value) and the deviation from that average, yield valuable information about the interaction that is of fundamental importance [19-22] without the need for carrying out large-dimensional matrix diagonalizations and with little to no limitations due to the dimensionality of the vector space. Likewise, this information can be propagated beyond the definition two-nucleon system to nuclei with larger numbers of nucleons [17,23]. Note that if one were to include higher-order energy moments, one would gradually obtain more detailed results that, in principle, would eventually reproduce those of a conventional microscopic calculations.

From a geometrical perspective, in spectral distribution theory every interaction is associated with a vector and the correlation coefficient define the angle (via a normalized scalar product) between two vectors. Hence, a correlation coefficient gives the normalized projection of one interaction ( $H$ ) onto another ( $H'$ ), while its square yields the percentage of  $H$  that reflect the characteristic properties of the  $H'$  interaction. The significance of a positive correlation coefficient is given by Cohen [24] and later revised to Table III.

In order to understand the nucleon-nucleon interaction at a more fundamental level and the ways the symmetries amplified in many-body nuclear dynamics are tied to the few-nucleon systems, we study the symplectic symmetry structure of the JISP16 realistic interaction. Specifically, we evaluate the correlation coefficient of the realistic interaction with the most general one- and two-body dynamically  $\text{Sp}(3, \mathbb{R})$ -symmetric interaction for a two-nucleon system, which is built as bilinear products of the 21  $\text{Sp}(3, \mathbb{R})$  generators together with the spin operator of the complementary  $\text{SU}(2)$  symmetry,

$$H_{Sp} = \sum_{i,j,o} c_{ij}^o \left[ X_{S_i}^{(\lambda_i \mu_i)} \times Y_{S_j}^{(\lambda_j \mu_j)} \right]_{(L_o S_o) J_o=0, M_o=0}, \quad (3)$$

TABLE III. Interpretation of a correlation coefficient

trivial	small	medium	large	very large	nearly perfect	perfect
0.00-0.09	0.10-0.29	0.30-0.49	0.50-0.69	0.70-0.89	0.90-0.99	1.00

TABLE IV. Correlation coefficient of the  $Sp(3, \mathbb{R})$ -preserving interaction with the  $T = 1$  part of the effective JISP16 and CD-Bonn realistic interactions (4 shells) together with pairing interaction for two nucleons occupying the shell regions specified by the oscillator shell  $l$  orbital momenta.

Interaction	s,p - s,p	sd - s,p	sd - sd	pf - s,p	pf - sd	pf - pf
JISP16	0.91	0.79	0.91	0.83	0.67	0.84
CD-Bonn	0.88	0.82	0.90	0.79	0.63	0.83
Pairing	0.62	0.24	0.41	0.28	0.12	0.24

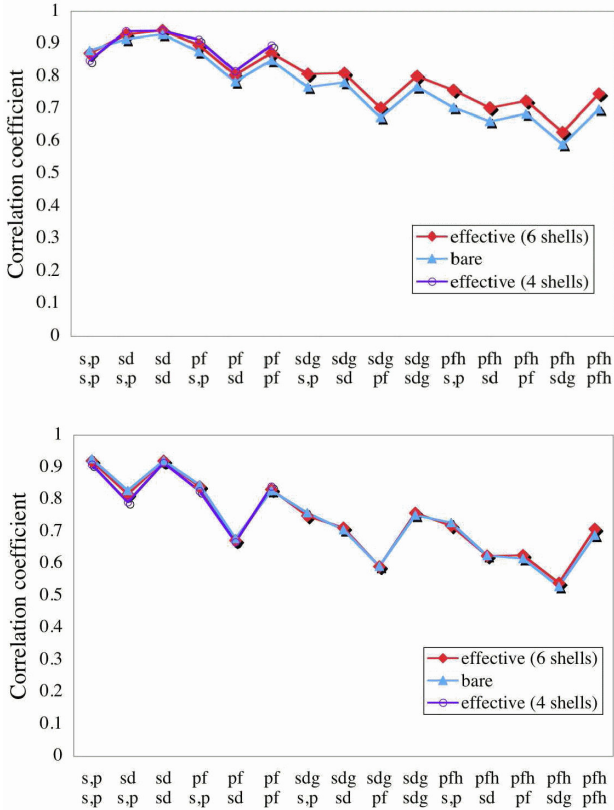


FIGURE 2. Correlation coefficient of the  $Sp(3, \mathbb{R})$ -preserving interaction with the bare and effective JISP16 realistic interactions for two nucleons in the shell regions specified along the  $x$  axis for isospin  $T = 0$  (upper panel) and  $T = 1$  (lower panel).

namely  $X$  ( $Y$ ) is either one of the  $Sp(3, \mathbb{R})$  generators ( $A^{(20)}$ ,  $B^{(02)}$ ,  $C^{(11)}$ , and  $H^{(00)}$  (1)), the spin operator with  $(\lambda \mu) = (00)$ , or the unity operator. Note that the many-particle kinetic energy, the harmonic oscillator Hamiltonian, the quadrupole-quadrupole interaction, as well as  $2\hbar\Omega$  and  $4\hbar\Omega$  monopole and quadrupole excitations straightforwardly enter into this Hamiltonian. The  $c_{ij}^o$  interaction strengths in Eq. 3 are determined in the framework of the spectral distribution theory as the projection of the realistic interaction onto the corresponding term

$$\left[ X_{S_i}^{(\lambda_i \mu_i)} \times Y_{S_j}^{(\lambda_j \mu_j)} \right]_{(L_o S_o) J_o=0, M_o=0}^{(\lambda_o \mu_o)}$$

and hence are not adjustable parameters. We examine the bare JISP16 interaction and its renormalized effective interaction for  $\hbar\Omega = 15$  MeV and up to the  $pf$  (4 shells) or  $pfh$  (6 shells) shells (Fig. 2). The results reveal correlation coefficient with the  $H_{Sp}$  (3) that range from  $\sim 0.6$  (typically regarded as a large correlation [25]) up to 0.94 (nearly perfect correlation). Interactions that are found to strongly correlate with each other are expected to produce energy spectra of a similar pattern as illustrated in Refs. 26 and 27.

Overall, more than 50% up to  $\sim 90\%$  of the  $T = 0$  and  $T = 1$  JISP16 interaction is accounted for by the symplectic dynamical symmetry interaction (Fig. 2). The correlation of the  $H_{Sp}$  symmetry-preserving Hamiltonian with the realistic interaction only changes slightly after the renormalization of the bare interaction, especially for the  $T = 1$  part. As well, the correlation is almost independent whether the renormalization is performed within different model space sizes, namely, truncated up to the  $pf$  shell or the  $pfh$  shell.

For comparative purposes, the same analysis was done for the effective CD-Bonn interaction, and as shown in Table IV the results track very closely with the results for the JISP16 effective interaction; that is, the CD-Bonn interaction is also strongly correlated with the  $H_{Sp}$  symmetry-preserving Hamiltonian (3), with the correlation being in “lock-step” with that of the JISP16 interaction. In contrast, a simplified interaction such as the pairing interaction displays a weak correlation when projected onto  $H_{Sp}$  (Table IV). The results show that the small symplectic symmetry breaking is not unique to the JISP16 interaction as it is observed for the CD-Bonn as well, even though some fine features of these interactions may differ. In addition, large correlations with the  $Sp(3, \mathbb{R})$ -preserving Hamiltonian are not typical, with the pairing interaction being a counter example. However, the nonzero correlation between the  $H_{Sp}$  and the pairing interaction is itself an interesting result as it suggests that pairing correlations are partially reflected in the  $H_{Sp}$  (3).

In agreement with the results from spectral distribution theory, the tensor decomposition of the bare and effective ( $\hbar\Omega = 15$  MeV) JISP16 realistic interaction reveals the dominance of the (00)  $SU(3)$  tensor interaction followed by (20) and (02) with  $L = 0$  angular momentum. Indeed, thirteen of the 21 symplectic generators have the same three  $SU(3)$  tensor characters and can construct one- and two-body (00), (20), and (02)  $L = 0$  terms in the  $Sp(3, \mathbb{R})$  symmetric microscopic interaction. In short, this study reveals symplectic symmetry properties of the nuclear force traced down to realistic interactions and together with the results deduced from the projection of realistic NCSM eigenstates onto the  $Sp(3, \mathbb{R})$ -symmetric basis provides the first evidence for the preponderance of the symplectic symmetry in nuclear many-body dynamics emerging from an *ab initio* theory.

## Acknowledgments

Discussions with Bruce R. Barrett are gratefully acknowledged. This work was supported by the US National Sci-

ence Foundation, Grants 0140300 and 0500291, and the Southeastern Universities Research Association, as well as, in part, by the US Department of Energy Grant DE-FG02-

87ER40371. T.D. acknowledges supplemental support from the Graduate School of Louisiana State University.

- i* We denote a  $N\hbar\Omega$   $kp$ - $kh$   $Sp(3, \mathbb{R})$  irrep as a symplectic irrep constructed as a multi-shell (vertical) cone of single- and multi-particle excitations over a  $N\hbar\Omega$   $k$ -particle- $k$ -hole symplectic bandhead. This notation is in accordance with the classification of symplectic irreps by their bandheads.
1. D.R. Peterson and K.T. Hecht, *Nucl. Phys. A* **344** (1980) 361.
  2. G. Rosensteel and D.J. Rowe, *Ann. Phys. (NY)* **126** (1980) 343.
  3. J.P. Draayer, K.J. Weeks, and G. Rosensteel, *Nucl. Phys. A* **413** (1984) 215.
  4. J. Escher and A. Leviatan, *Phys. Rev. C* **65** (2002) 054309.
  5. F. Arickx, J. Broeckhove, and E. Deumens, *Nucl. Phys. A* **377**(1982) 121.
  6. S.S. Avancini and E.J.V. de Passos, *J. Phys. G* **19** (1993) 125.
  7. D.J. Rowe, G. Thiamova, and J.L. Wood, *Phys. Rev. Lett.* **97** (2006) 202501.
  8. T. Dytrych, K.D. Sviratcheva, C. Bahri, J.P. Draayer, and J.P. Vary, *Phys. Rev. Lett.* **98** (2007) 162503.
  9. K.T. Hecht, *J. Phys. Soc. Japan* **44** Suppl. (1978) 232; K.T. Hecht and D. Braunschweig, *Nucl. Phys. A* **295** (1978) 34; Y. Suzuki, *Nucl. Phys. A* **448** (1986) 395; Y. Suzuki and K.T. Hecht, *Nucl. Phys. A* **455** (1986) 315; Y. Suzuki and S. Hara, *Phys. Rev. C* **39** (1989) 658.
  10. G. Rosensteel and D.J. Rowe, *Phys. Rev. Lett.* **38** (1977) 10; G. Rosensteel and D.J. Rowe, *Ann. Phys. (N.Y.)* **126** (1980) 343; D.J. Rowe, *Rep. Prog. Phys.* **48** (1985) 1419.
  11. O. Castaños, J.P. Draayer, and Y. Leschber, *Z. Phys. A* **329** (1988) 33.
  12. A. Bohr and B.R. Mottelson, *Mat. Fys. Medd. Dan. Vid. Selsk.* **27** (1953) 16.
  13. J.P. Vary, "The Many-Fermion-Dynamics Shell-Model Code," Iowa State University 1992 (unpublished); J.P. Vary and D.C. Zheng, *ibid* 1994 (unpublished).
  14. A.M. Shirokov, A.I. Mazur, S.A. Zaytsev, J.P. Vary, and T.A. Weber, *Phys. Rev. C* **70** (2004) 044005; A.M. Shirokov, J.P. Vary, A.I. Mazur, S.A. Zaytsev, and T.A. Weber, *Phys. Letts. B* **621** (2005) 96; A.M. Shirokov, J.P. Vary, A.I. Mazur, and T.A. Weber, *Phys. Letts. B* **644** (2007) 33.
  15. T. Dytrych, K.D. Sviratcheva, C. Bahri, J.P. Draayer, and J.P. Vary, *Phys. Rev. C* **76** (2007) 014315.
  16. J.B. French and K.F. Ratcliff, *Phys. Rev. C* **3** (1971) 94.
  17. F.S. Chang, J.B. French, and T.H. Thio, *Ann. Phys. (N.Y.)* **66** (1971) 137.
  18. J.B. French, V.K.B. Kota, A. Pandey, and S. Tomsovic, *Ann. Phys. (N.Y.)* **181** (1988) 235; V.K.B. Kota and D. Majumdar, *Z. Phys. A* **351** (1995) 365; *Z. Phys. A* **351** (1995) 377; S. Tomsovic, M.B. Johnson, A. Hayes, and J.D. Bowman, *Phys. Rev. C* **62** (2000) 054607; J.M.G. Gomez, K. Kar, V.K.B. Kota, R.A. Molina, and J. Retamosa, *Phys. Lett. B* **567** (2003) 251; M. Horoi, M. Ghita, and V. Zelevinsky, *Phys. Rev. C* **69** (2004) 041307(R); N.D. Chavda, V. Potbhare, and V.K. B. Kota, *Phys. Lett. A* **326** (2004) 47; Y.M. Zhao, A. Arima, N. Yoshida, K. Ogawa, N. Yoshinaga, and V.K.B. Kota, *Phys. Rev. C* **72** (2005) 064314.
  19. V. Potbhare, *Nucl. Phys. A* **289** (1977) 373.
  20. T.R. Halemane, K. Kar, and J.P. Draayer, *Nucl. Phys. A* **311** (1978) 301.
  21. C.R. Countee, J.P. Draayer, T.R. Halemane, and K. Kar, *Nucl. Phys. A* **356** (1981) 1.
  22. J.P. Draayer and G. Rosensteel *Phys. Lett. B* **124** (1983) 281; G. Rosensteel and J.P. Draayer, *Nucl. Phys. A* **436** (1985) 445.
  23. K.T. Hecht and J.P. Draayer, *Nucl. Phys. A* **223** (1974) 285.
  24. J. Cohen, P. Cohen, S.G. West, and L.S. Aiken, *Applied multiple regression/correlation analysis for the behavioral sciences*, 2nd ed. (Lawrence Erlbaum Associates, Hillsdale, New Jersey, 2003).
  25. G. Rosensteel, *Nucl. Phys. A* **341** (1980) 397.
  26. K.D. Sviratcheva, J.P. Draayer, and J.P. Vary, *Phys. Rev. C* **73** (2006) 034324.
  27. K.D. Sviratcheva, J.P. Draayer, and J.P. Vary, *Nucl. Phys. A* **786** (2007) 31.